Weyl Points in Three-Dimensional Optical Lattices: Synthetic Magnetic Monopoles in Momentum Space

Tena Dubček,[1] Colin J. Kennedy,[2] Ling Lu,[2] Wolfgang Ketterle,[2] Marin Soljačić,[2] and Hrvoje Buljan[1]
[1]Department of Physics, University of Zagreb, Bijenička cesta 32, 10000 Zagreb, Croatia
[2]Department of Physics, Massachusetts Institute of Technology, Cambridge, Massachusetts 02139, USA
(Received 24 December 2014; published 3 June 2015)

We show that a Hamiltonian with Weyl points can be realized for ultracold atoms using laser-assisted tunneling in three-dimensional optical lattices. Weyl points are synthetic magnetic monopoles that exhibit a robust, three-dimensional linear dispersion, identical to the energy-momentum relation for relativistic Weyl fermions, which are not yet discovered in particle physics. Weyl semimetals are a promising new avenue in condensed matter physics due to their unusual properties such as the topologically protected "Fermi arc" surface states. However, experiments on Weyl points are highly elusive. We show that this elusive goal is well within experimental reach with an extension of techniques recently used in ultracold gases.

DOI: 10.1103/PhysRevLett.114.225301 PACS numbers: 67.85.-d, 03.65.Vf, 03.75.Lm

In relativistic quantum field theory there are three types of fermions: Dirac, Majorana, and Weyl fermions [1]. The latter two have never been observed. It was conjectured that neutrinos could be Weyl fermions before the discovery of neutrino oscillations ruled out such a possibility. Nowadays, there is a great excitement on Weyl semimetals: gapless topological states of matter with bulk low-energy electrons behaving as Weyl fermions, and intriguing "Fermi arc" topological surface states [2–4]. Besides the fundamental importance of Weyl fermions and related phenomena such as the Adler-Bell-Jackiw chiral anomaly, the topological surface states of Weyl semimetals also hold great potential for applications [3]. These systems followed the development of topological insulators [5,6], emphasizing the role of band topology in describing exotic phases of matter. However, experiments on Weyl fermions are highly elusive.

Recent experiments on synthetic magnetic fields in ultracold atomic gases [7–17], alongside advances in photonics [18–24], have propelled these systems as promising platforms for investigating topological effects and novel states of matter (see Refs. [25–29] for reviews). However, Weyl points have been scarcely addressed in these fields [24,30–33]. In photonics, a double gyroid photonic crystal with broken time reversal and/or parity symmetry was predicted to have Weyl points [24]. Theoretical lattice models possessing Weyl points [30,32,33], and Weyl spin-orbit coupling [31], were studied in the context of ultracold atomic gases. Because of the elusive nature of Weyl fermions, a viable and possibly simple scheme for their experimental realization in ultracold atomic gases would be of great importance, exploiting advantages of atomic systems to contribute to Weyl physics research across disciplines.

Here, we propose the realization of the Weyl Hamiltonian for ultracold atoms in a straightforward modification of the experimental system that was recently employed to obtain the Harper Hamiltonian [12]. As an example of phenomena inherent to Weyl points, but most suitable for observing in ultracold systems, we discuss the unique spherical-shell expansion of a Bose-Einstein condensate (BEC), by initially exciting eigenmodes close to the Weyl point.

The Harper [34] (also referred to as the Hofstadter [35]) Hamiltonian was recently realized in optical lattices in the MIT [12] and Munich [13] groups, by employing laser-assisted tunneling to create synthetic magnetic fields. Historically, the first synthetic magnetic fields were implemented in rapidly rotating BECs by using Coriolis forces [7,8]. The first implementation using laser-atom interactions was in the NIST group with spatially dependent Raman optical coupling between internal hyperfine atomic states in bulk BECs [9]. Methods of generating synthetic magnetic fields used in optical lattices engineer the complex tunneling parameters between lattice sites [11–13]. They include shaking of the optical lattice, as demonstrated in the Hamburg group [11], laser-assisted tunneling which realized staggered magnetic fields in optical superlattices [10] and the Harper Hamiltonian in tilted lattices [12,13], and an all-optical scheme which enables flux rectification in optical superlattices [14]. One of the intriguing recent achievements is the realization of Dirac monopoles in a synthetic magnetic field produced by a bulk spinor BEC [16]. It should be emphasized that all lattices with nontrivial topology that were experimentally realized so far were in one or two dimensions. This work points out how a straightforward inclusion of the third dimension enables experiments on intriguing and elusive topological phenomena.

The laser-assisted tunneling scheme [10,12,13] requires only far off-resonant lasers and a single atomic internal state, and thus avoids heating by spontaneous emission. An early related proposal involved coupling of different internal states [36]. The scheme used here is based on the proposal introduced in Ref. [37], and later modified to enable generation of a homogeneous field [12,13]. With

this scheme, we can engineer both the amplitude and phase of the tunneling matrix elements in optical lattices. For example, if a cubic D-dimensional optical lattice has tunneling matrix elements J_d $(d = 1, \ldots, D)$, laser-assisted tunneling can, in principle, change them to $K_d e^{i\Phi_d}$, where the phases depend on the position.

For Weyl points to occur, time reversal and/or inversion symmetry must be broken [3,24]. The two-dimensional (2D) lattice realized in Ref. [12], which is our starting point, possesses both symmetries. Tunneling along the x direction is laser assisted, with the phase alternating between 0 and π, whereas hopping along y stays regular [see Fig. 1(a)]. The centers of inversion symmetry are denoted by orange crosses in Fig. 1(a). The time-reversal symmetry is a consequence of the fact that the accumulated phase per plaquette π is equivalent to a phase of $-\pi$. This system is a realization of the Harper Hamiltonian for $\alpha = 1/2$, where α is the flux per plaquette in units of the flux quantum [12,13]. The lattice has two sublattices $(A - B)$ giving rise to pseudospin. In quasimomentum representation, the Hamiltonian is $H_{\alpha=1/2}(\mathbf{k}) = -2\{J_y \cos(k_y a)\sigma_x + K_x \sin(k_x a)\sigma_y\}$, where σ_i denote Pauli matrices; it has two bands, $E_{\alpha=1/2} = \pm 2\sqrt{K_x^2 \sin^2(k_x a) + J_y^2 \cos^2(k_y a)}$,

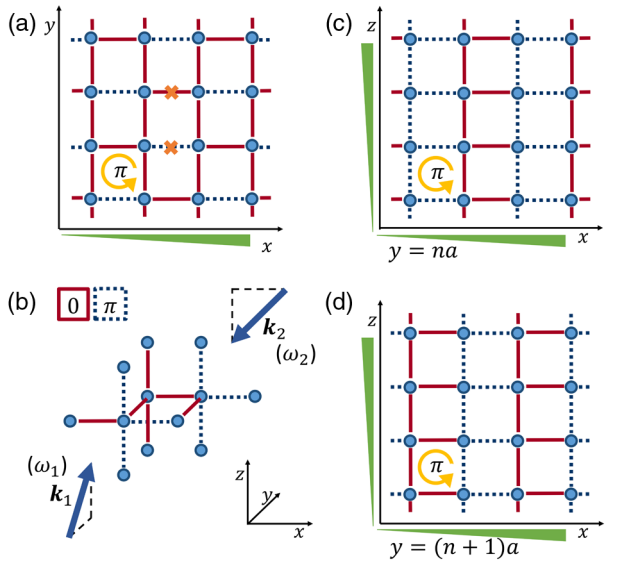

FIG. 1 (color online). Sketch of the 3D cubic lattice with phase engineered hopping along x and z directions, which possesses Weyl points in momentum space. Dashed (solid) lines depict hopping with acquired phase π (0, respectively). (a) The xy planes of the lattice are equivalent to the lattice of the Harper Hamiltonian for $\alpha = 1/2$. Centers of inversion symmetry for this 2D lattice are denoted by orange crosses. Green triangles along the axes denote the tilted directions. (b) A pair of Raman lasers enabling laser-assisted tunneling is sketched with arrows. The 3D lattice can be visualized as alternating stacks of 2D lattices parallel to the xz plane, which are shown in (c) and (d); the hopping between these planes (along y) is regular. The hopping along z is alternating with phases 0 or π, depending on the position in the xy plane [see (b), (c), and (d)], which breaks the inversion symmetry.

touching at two 2D Dirac points at $(k_x, k_y) = (0, \pm\pi/2a)$ in the Brillouin zone [38]. Here (K_x, J_y) denote the tunneling amplitudes, and (k_x, k_y) the Bloch wave vector.

Suppose that we construct a 3D lattice by stacking 2D lattices from Fig. 1(a), one on top of each other, with regular hopping (J_z) along the third (z) direction. This 3D lattice is described by the Hamiltonian

$$H_{\mathrm{LN}}(\mathbf{k}) = -2\{J_y \cos(k_y a)\sigma_x + K_x \sin(k_x a)\sigma_y + J_z \cos(k_z a)\mathbb{1}\}, \quad (1)$$

where $\mathbb{1}$ is the unity matrix. The 2D Dirac points have become line nodes (LN) in the 3D Brillouin zone at which the two bands touch: $E_{\mathrm{LN}} = -2J_z \cos(k_z a) \pm 2\sqrt{K_x^2 \sin^2(k_x a) + J_y^2 \cos^2(k_y a)}$. Note that both the inversion and the time-reversal symmetry are inherited from the $\alpha = 1/2$ Harper Hamiltonian. In order to achieve Weyl points, we must break one of these when adding the third dimension.

To this end, we propose to construct a 3D cubic lattice with laser-assisted tunneling along both x and z directions as follows. First, tunneling along these directions is suppressed by introducing a linear tilt of energy Δ per lattice site, identical along x and z. It can be obtained by a linear gradient potential (e.g., gravity or magnetic field gradient [12]) along the $\hat{x} + \hat{z}$ direction. The tunneling is restored by two far-detuned Raman beams of frequency detuning $\delta\omega = \omega_1 - \omega_2$, and momentum difference $\delta\mathbf{k} = \mathbf{k}_1 - \mathbf{k}_2$ [12]. For resonant tunneling, $\delta\omega = \Delta/\hbar$, and a sufficiently large tilt $(J_x, J_z \ll \Delta \ll E_{\mathrm{gap}})$ [12], time averaging over the rapidly oscillating terms yields an effective 3D Hamiltonian

$$H_{\mathrm{3D}} = -\sum_{m,n,l} (K_x e^{-i\Phi_{m,n,l}} a^\dagger_{m+1,n,l} a_{m,n,l} + J_y a^\dagger_{m,n+1,l} a_{m,n,l} + K_z e^{-i\Phi_{m,n,l}} a^\dagger_{m,n,l+1} a_{m,n,l} + \mathrm{H.c.}). \quad (2)$$

Here, $a^\dagger_{m,n,l}$ $(a_{m,n,l})$ is the creation (annihilation) operator on the site (m, n, l), and $\Phi_{m,n,l} = \delta\mathbf{k} \cdot \mathbf{R}_{m,n,l} = m\Phi_x + n\Phi_y + l\Phi_z$ are the nontrivial hopping phases, dependent on the positions $\mathbf{R}_{m,n,l}$. An inspection of Eq. (2) reveals that a wealth of energy dispersion relations can be achieved by manipulating the directions of Raman lasers $\delta\mathbf{k}$. Next, we choose the directions of the Raman lasers such that $(\Phi_x, \Phi_y, \Phi_z) = \pi(1, 1, 2)$, i.e., $\Phi_{m,n,l} = (m + n)\pi$ (modulo 2π). This is schematically illustrated in Fig. 1(b). It should be noted that a seemingly equivalent choice, $(\Phi_x, \Phi_y, \Phi_z) = \pi(1, 1, 0)$, will not be operational, because a *nonvanishing* momentum transfer in the tilt direction is necessary for the resonant tunneling to be restored [12,13,38].

A sketch of the 3D lattice obtained with such a choice of phases is illustrated in Fig. 1. It can be thought of as an alternating stack of two types of 2D lattices, parallel to the

xz plane, which are illustrated in Figs. 1(c) and 1(d); hopping between these planes is regular (along y). The 3D lattice has two sublattices (A-B). Another view is the stacking of 2D lattices described by the Harper Hamiltonian $H_{\alpha=1/2}$ [Fig. 1(a)], such that the hopping along z has phases 0 or π, for $m+n$ even or odd, respectively. This breaks the inversion symmetry, and under application of Bloch's theorem,

$$H(\mathbf{k}) = -2\{J_y \cos(k_y a)\sigma_x + K_x \sin(k_x a)\sigma_y - K_z \cos(k_z a)\sigma_z\}. \quad (3)$$

Mathematically, the chosen phase engineering along z has replaced the identity matrix in H_{LN} with the Pauli matrix σ_z.

The energy spectrum of the Hamiltonian has two bands,

$$E(\mathbf{k}) = \pm 2\sqrt{K_x^2 \sin^2(k_x a) + J_y^2 \cos^2(k_y a) + K_z^2 \cos^2(k_z a)}, \quad (4)$$

which touch at four Weyl points within the first Brillouin zone at $(k_x, k_y, k_z) = (0, \pm\pi/2a, \pm\pi/2a)$. Figure 2 depicts the energy spectra in the first Brillouin zone, the Weyl points, and their chiralities. The dispersions around Weyl points are locally linear and described by the anisotropic Weyl Hamiltonian $H_W(\mathbf{q}) = \sum_{i,j} q_i \nu_{ij} \sigma_j$ [4], where $\mathbf{q} = \mathbf{k} - \mathbf{k}_W$ is the displacement vector from the Weyl point (located at $\mathbf{k}_W$) in momentum space. Here $[v_{ij}]$ is a 3×3 matrix, with elements $v_{xy} = -2K_x a$, $v_{yx} = \pm 2J_y a$, $v_{zz} = \pm 2K_z a$, and zero otherwise. The topological nature of the system is reflected in the possibility to assign (positive and negative) chirality, defined as $\kappa = \mathrm{sign}(\det[v_{ij}])$, to the Weyl points [24].

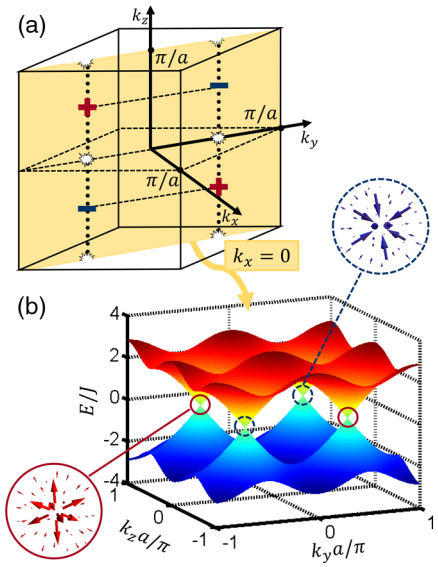

FIG. 2 (color online). Sketch of the first Brillouin zone of the lattice depicted in Fig. 1, energy spectrum and Weyl points. (a) The positions of the Weyl points in the Brillouin zone and their chiralities are indicated with + and − signs. If a tunable A-B sublattice energy offset is introduced, Weyl points move along dotted lines, and can annihilate at points denoted with stars (see text). (b) Energy spectrum in the $k_x = 0$ plane [shaded plane in (a)] shows linear dispersion in the proximity of the Weyl points. The insets show the Berry curvature of two Weyl points, demonstrating that they are synthetic magnetic monopoles in momentum space.

Weyl points are monopoles of the synthetic magnetic field in momentum space. In order to verify this property of our energy nodes, we have calculated the gauge field, i.e., Berry connection $\mathbf{A}(\mathbf{k}) = i\langle u(\mathbf{k})|\nabla_{\mathbf{k}}|u(\mathbf{k})\rangle$, and the synthetic magnetic field, i.e., Berry curvature $\mathbf{B} = \nabla_{\mathbf{k}} \times \mathbf{A}(\mathbf{k})$. The obtained Berry curvature is depicted in the insets of Fig. 2, clearly demonstrating that what we have proposed is a construction of topological synthetic magnetic monopoles in the momentum space of a 3D optical lattice.

These monopoles are robust to any perturbation which adds a σ_i term ($i = x, y, z$) to the Hamiltonian. The only way for Weyl points to disappear is when two of them with opposite chirality annihilate (see Supplemental Material [39]). This topologically protected nature of Weyl points can be probed in the proposed setup by adding a tunable A-B sublattice energy offset in the same fashion as in Ref. [15], such that the on-site energy at sites with $m+n$ odd (even) is ϵ ($-\epsilon$). This adds an $\epsilon\sigma_z$ term to the Hamiltonian in Eq. (3), and shifts the Weyl points parallel to the z axis by tuning ϵ, as illustrated in Fig. 2(a). By making this term large enough ($\epsilon = \pm 2K_z$), one can drive the annihilation of the Weyl points pairwise either at $(k_x = 0, k_y = \pm\pi/2a, 0)$ for $\epsilon = -2K_z$, or at the edge of the Brillouin zone for $\epsilon = 2K_z$, and open up a gap in the system.

Now that we have identified the scheme which creates the Weyl Hamiltonian, we propose schemes for their experimental detection which are applicable for both ultracold bosons and fermions. In order to verify that we have points at which the two bands touch in the 3D Brillouin zone, one can accelerate the initially prepared ultracold atomic cloud from the ground state position in momentum space towards the Weyl point using a constant force, and observe the crossover to the second band which can be revealed by time-of-flight measurements. By pushing the cloud in directions which would "miss" the Weyl point, Bloch oscillations would be observed within the lowest band. Such a scheme was recently used to detect Dirac points in a honeycomb optical lattice [42], and also to probe the topological phase transition in the Haldane model [15]. Two points are worth emphasizing here. First, Weyl points are robust and would not be destroyed by an additional small force [3,29,39]. Second, the trajectory of the gas being pushed would not be deflected in our lattice, because we have a time-reversal symmetric Hamiltonian.

The second scheme to observe the Weyl points is Bragg spectroscopy [43]. By using an additional pair of Raman lasers, i.e., a two-photon Raman transition, one can couple

states of the Hamiltonian (3) with a given energy and momentum difference, and induce excitations from the lower band to the upper band to probe the band structure [43]. This scheme would reveal the existence of Weyl points with very high resolution as it would not change the internal atomic state, and therefore not be sensitive to Zeeman shifts.

The proposed methods are applicable for both bosons and fermions. Here we discussed atoms in a single spin state; however, a mixture of spin states provides another degree of freedom to explore new phenomena, e.g., see [44]. By using single spin fermions, the Weyl semimetal phase could be achieved by adjusting the particle density, i.e., the Fermi level to the energy of the Weyl points.

Realization of Weyl points with ultracold atoms would open a new frontier of research in Weyl physics, with potential to exploit unique atomic physics methods of state preparation and diagnostics. As an example, consider a BEC which is initially formed in the ground state of the band structure (e.g., see [17]), and then, by applying either a potential tilt or a Bragg pulse of finite duration, placed (in quasimomentum space) at a Weyl point. This state is a superposition of eigenstates from the vicinity of the Weyl point, and would start expanding in our 3D lattice (see Supplemental Material [39]). If we assume isotropic dispersion around Weyl points ($K_x \approx J_y \approx K_z$), the magnitude of the group velocity $\hbar^{-1}|\nabla_{\mathbf{k}} E(\mathbf{k})|$ is uniform. In this case, the BEC has unique expansion in a form of a spherical shell with radius $\sim\hbar^{-1}|\nabla_{\mathbf{k}} E(\mathbf{k})|t$ (the shell would have structure depending on the initial excitation [39–41]).

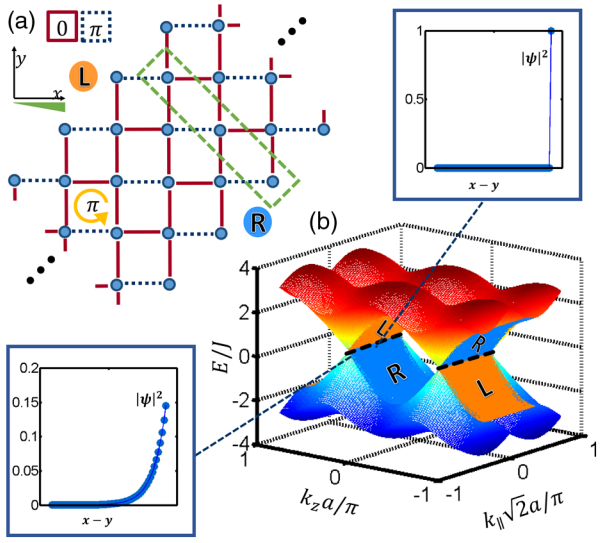

FIG. 3 (color online). Surface states and Weyl points. (a) A slab of finite width is cut from the 3D lattice along planes orthogonal to the $\hat{x} - \hat{y}$ direction; cross section in the xy plane is sketched. The two sides of the slab are indicated with letters L and R. (b) Energy spectrum of the slab. The two dispersion sheets of surface states (corresponding to the two surfaces of the slab) are denoted with R (blue) and L (orange). The intersections of the two sheets are Fermi arcs (denoted with dashed lines). The arcs connect Weyl points of opposite chiralities. The insets show examples of the profile of the Fermi arc surface states across the slab, as indicated by the green dashed box in (a).

Weyl semimetals imply the existence of intriguing topological surface states that come in the form of Fermi arcs in momentum space [3]. Topological effects such as Berry curvature have been experimentally observed in ultracold atomic systems [14,15]. However, surface states are difficult to detect with light scattering methods because one has to distinguish them from the bulk signal (e.g., see [45] and references therein). Nevertheless, it is illustrative to show Fermi arcs and surface states in our model. In Fig. 3(a) we take a slab of our lattice cut orthogonally to the $\hat{x} - \hat{y}$ direction (infinite along the $\hat{z}$ and $\hat{x} + \hat{y}$ directions), and in Fig. 3(b) we plot the energy spectrum of this slab $E(\mathbf{k})$, where $\mathbf{k} = k_\parallel(\hat{x} + \hat{y})/\sqrt{2} + k_z\hat{z}$ (see Supplemental Material [39] for details). The Weyl points are now connected with Fermi arcs in momentum space (shown with dashed lines). The states on the arcs are surface states [3], as can be seen from the inset in Fig. 3(b) (only states from one of the surfaces are shown). Surface states closer to the Weyl points spread more into the bulk than those in the center of the arcs. The Fermi arcs belong to two energy dispersion sheets of surface states, each one corresponding to one of the slab surfaces. The two sheets are located adjacent to the energy dispersion of bulk states [3]; one sheet is on the bottom (the other is on the top) of the upper (lower, respectively) band. These two sheets intersect at Fermi arcs.

In conclusion, we pointed out that Weyl points, and all of the exciting phenomena that they include, could be experimentally addressed in the setup that was recently employed to obtain the Harper Hamiltonian [12,13]. Without phase engineered hopping methods, which are well developed in atomic systems, the creation of Weyl points is more demanding, possible only for a reduced number of space groups and points of symmetry in the Brillouin zone [46]. An interesting venue would be to include interactions between the atoms [17], which can fundamentally change the system's behavior (for an example, consider the interaction induced phase transition to a topological insulator in a fermionic 2D optical lattice [47]). Given the fact that experiments on Weyl points and Weyl fermions are elusive, fundamentally important, and within reach in optical lattices, this can open a new frontier of Weyl physics research.

This work was supported by the Unity through Knowledge Fund (UKF Grant No. 5/13), the NSF through the Center for Ultracold Atoms, by NSF Grant No. PHY-0969731, and an AFOSR MURI, and in part by the U.S. Army Research Laboratory and the U.S. Army Research Office through the Institute for Soldier Nanotechnologies, under Contract No. W911NF-13-D-0001. We are grateful to Cody Burton, Woo Chang Chung, Liang Fu, John D. Joannopoulos, Krešimir Kumerički, Mario Novak, Juraj Radić, Ivica Smolić, Ashvin Vishwanath, and Martin Zwierlein for useful discussions.

Note added.—After this work was submitted, a few papers appeared claiming observation of Weyl points [48], and Weyl semimetal phase [49,50].

[1] H. Weyl, Z. Phys. **56**, 330 (1929).
[2] X. Wan, A. M. Turner, A. Vishwanath, and S. Y. Savrasov, Phys. Rev. B **83**, 205101 (2011).
[3] A. M. Turner and A. Vishwanath, arXiv:1301.0330.
[4] P. Hosur and X. Qi, C.R. Phys. **14**, 857 (2013).
[5] C. L. Kane and E. J. Mele, Phys. Rev. Lett. **95**, 226801 (2005).
[6] M. Z. Hasan and C. L. Kane, Rev. Mod. Phys. **82**, 3045 (2010).
[7] K. W. Madison, F. Chevy, W. Wohlleben, and J. Dalibard, Phys. Rev. Lett. **84**, 806 (2000).
[8] J. R. Abo-Shaeer, C. Raman, J. M. Vogels, and W. Ketterle, Science **292**, 476 (2001).
[9] Y-J. Lin, R. L. Compton, K. Jiménez-García, J. V. Porto, and I. B. Spielman, Nature (London) **462**, 628 (2009).
[10] M. Aidelsburger, M. Atala, S. Nascimbene, S. Trotzky, Y.-A. Chen, and I. Bloch, Phys. Rev. Lett. **107**, 255301 (2011).
[11] J. Struck, C. Ölschläger, M. Weinberg, P. Hauke, J. Simonet, A. Eckardt, M. Lewenstein, K. Sengstock, and P. Windpassinger, Phys. Rev. Lett. **108**, 225304 (2012).
[12] H. Miyake, G. A. Siviloglou, C. J. Kennedy, W. C. Burton, and W. Ketterle, Phys. Rev. Lett. **111**, 185302 (2013).
[13] M. Aidelsburger, M. Atala, M. Lohse, J. T. Barreiro, B. Paredes, and I. Bloch, Phys. Rev. Lett. **111**, 185301 (2013).
[14] M. Aidelsburger, M. Lohse, C. Schweizer, M. Atala, J. T. Barreiro, S. Nascimbene, N. R. Cooper, I. Bloch, and N. Goldman, Nat. Phys. **11**, 162 (2015).
[15] G. Jotzu, M. Messer, R. Desbuquois, M. Lebrat, T. Uehlinger, D. Greif, and T. Esslinger, Nature (London) **515**, 237 (2014).
[16] M. W. Ray, E. Ruokokoski, S. Kandel, M. Mottonen, and D. S. Hall, Nature (London) **505**, 657 (2014).
[17] C. J. Kennedy, W. Cody Burton, W. Chang Chung, and W. Ketterle, arXiv:1503.08243.
[18] Z. Wang, Y. Chong, J. D. Joannopoulos, and M. Soljačić, Nature (London) **461**, 772 (2009).
[19] K. Fang, Z. Yu, and S. Fan, Nat. Photonics **6**, 782 (2012).
[20] J. M. Zeuner, N. K. Efremidis, R. Keil, F. Dreisow, D. N. Christodoulides, A. Tünnermann, S. Nolte, and A. Szameit, Phys. Rev. Lett. **109**, 023602 (2012).
[21] Y. E. Kraus, Y. Lahini, Z. Ringel, M. Verbin, and O. Zilberberg, Phys. Rev. Lett. **109**, 106402 (2012).
[22] M. C. Rechtsman, J. M. Zeuner, A. Tünnermann, S. Nolte, M. Segev, and A. Szameit, Nat. Photonics **7**, 153 (2013).
[23] M. Hafezi, S. Mittal, J. Fan, A. Migdall, and J. M. Taylor, Nat. Photonics **7**, 1001 (2013).
[24] L. Lu, L. Fu, J. D. Joannopoulos, and M. Soljačić, Nat. Photonics **7**, 294 (2013).
[25] J. Dalibard, F. Gerbier, G. Juzeliunas, and P. Öhberg, Rev. Mod. Phys. **83**, 1523 (2011).
[26] I. Bloch, J. Dalibard, and S. Nascimbene, Nat. Phys. **8**, 267 (2012).
[27] N. Goldman, G. Juzeliunas, P. Öhberg, and I. B. Spielman, Rep. Prog. Phys. **77**, 126401 (2014).
[28] I. Carusotto and C. Ciuti, Rev. Mod. Phys. **85**, 299 (2013).
[29] L. Lu, J. D. Joannopoulos, and M. Soljačić, Nat. Photonics **8**, 821 (2014).
[30] Z. Lan, N. Goldman, A. Bermudez, W. Lu, and P. Öhberg, Phys. Rev. B **84**, 165115 (2011).
[31] B. M. Anderson, G. Juzeliunas, V. M. Galitski, and I. B. Spielman, Phys. Rev. Lett. **108**, 235301 (2012).
[32] S. Ganeshan and S. Das Sarma, Phys. Rev. B **91**, 125438 (2015).
[33] J. H. Jiang, Phys. Rev. A **85**, 033640 (2012).
[34] P. G. Harper, Proc. Phys. Soc. London Sect. A **68**, 874 (1955).
[35] D. R. Hofstadter, Phys. Rev. B **14**, 2239 (1976).
[36] D. Jaksch and P. Zoller, New J. Phys. **5**, 56 (2003).
[37] A. R. Kolovsky, Europhys. Lett. **93**, 20003 (2011).
[38] H. Miyake, Ph.D. thesis, Massachusetts Institute of Technology, 2013.
[39] See Supplemental Material at http://link.aps.org/supplemental/10.1103/PhysRevLett.114.225301, which includes Refs. [3,40,41], for details and additional calculations regarding the spherical shell expansion of a BEC around a Weyl point and the appearance of Fermi arcs and surface states.
[40] O. Peleg, G. Bartal, B. Freedman, O. Manela, M. Segev, and D. N. Christodoulides, Phys. Rev. Lett. **98**, 103901 (2007).
[41] M. V. Berry, J. Opt. A **6**, 289 (2004).
[42] L. Tarruell, D. Greif, Th. Uehlinger, G. Jotzu, and T. Esslinger, Nature (London) **483**, 302 (2012).
[43] Ph. T. Ernst, S. Götze, J. S. Krauser, K. Pyka, Dirk-Soren Lühmann, D. Pfannkuche, and K. Sengstock, Nat. Phys. **6**, 56 (2010).
[44] C. J. Kennedy, G. A. Siviloglou, H. Miyake, W. C. Burton, and W. Ketterle, Phys. Rev. Lett. **111**, 225301 (2013).
[45] N. Goldman, J. Dalibard, A. Dauphin, F. Gerbier, M. Lewenstein, P. Zoller, and I. B. Spielman, Proc. Natl. Acad. Sci. U.S.A. **110**, 6736 (2013).
[46] J. L. Manes, Phys. Rev. B **85**, 155118 (2012).
[47] K. Sun, W. V. Liu, A. Hemmerich, and S. Das Sarma, Nat. Phys. **8**, 67 (2012).
[48] L. Lu *et al.*, arXiv:1502.03438.
[49] S.-Y. Xu *et al.*, arXiv:1502.03807.
[50] B. Q. Lv *et al.*, arXiv:1502.04684.

SUPPLEMENTAL MATERIAL

I. ROBUSTNESS OF WEYL POINTS

Weyl points are topologically protected. The only way for Weyl points to disappear is when two of them with opposite chirality annihilate [1]. This means that in the proposed experiment they will not be destroyed by a small perturbation of parameters. For example, suppose that in the experiment one does not direct the Raman lasers to get exactly $(\Phi_x, \Phi_y, \Phi_z) = \pi(1, 1, 2)$, but somewhat different values. Weyl points will still be present in the Brillouin zone, and could be observed with Bragg spectroscopy even for large perturbations. The other parts of the band structure would change. If the deviations from exact values of (Φ_x, Φ_y, Φ_z) become large, the proposed observation by pushing the BEC through Weyl points will be harder to achieve because of the changes in the band structure away from Weyl points.

II. SPHERICAL SHELL DIFFRACTION

Here we illustrate, by using an example, what happens when one excites eigenmodes in the vicinity of Weyl points, more specifically, in the region where linear energy-momentum relation holds. The time-dependent wave-function $\phi(\mathbf{r}, t)$, in continuous coordinates, can be written as a superposition of eigenmodes of the system:

$$\phi\left(\mathbf{r}, t\right) = \iiint dq_x dq_y dq_z \Phi_0\left(\mathbf{q}\right) e^{i\eta t\sqrt{q_x^2+q_y^2+q_z^2}} U_{\mathbf{q}} e^{i\mathbf{qr}}. \tag{1}$$

Here the coefficients $\Phi_0\left(\mathbf{q}\right)$ correspond to the projection of the initial wave function (at $t = 0$) on the eigenmodes, and the time dependent phases reflect the isotropic linear dispersion around the Weyl points, with $\eta = \pm 2Ja/\hbar$; for simplicity we assumed that hopping is identical in all directions, and $\mathbf{q} = \mathbf{k} - \mathbf{k}_W$ is the displacement vector from the Weyl point. For a sufficiently narrow distribution of eigenmodes, $U_{\mathbf{q}}$ can be approximated as all having the same amplitude $U_{\mathbf{q}=\mathbf{0}}$, where $\mathbf{q} = \mathbf{0}$ corresponds to the Weyl point. In the special, but illustrative case, where the initial distribution is exponential around the Weyl point, $\Phi_0(\mathbf{q}) = e^{-g\sqrt{q_x^2+q_y^2+q_z^2}}$, the integral can be solved analytically:

$$\phi\left(\mathbf{r}, t\right) \sim \frac{\left(g - i\eta t\right)}{\left(\left(g - i\eta t\right)^2 + \left(x^2 + y^2 + z^2\right)\right)^2}. \tag{2}$$

For sufficiently long time ($\eta t \gg g$), the corresponding wave function density propagates as a spherical shell of a constant width, whose velocity of propagation is readily found to be

$$v(t) = |\eta| \left(1 - \left(\frac{g}{\eta t}\right)^2\right)^{-1/2} \approx |\eta| \left(1 + \left(\frac{g}{\eta t}\right)^2 + ...\right). \quad (3)$$

This corresponds to the uniform group velocity close to the Weyl point: $\hbar^{-1}|\nabla_{\mathbf{k}} E(\mathbf{k})| = 2Ja/\hbar = |\eta|$.

A similar approach has been used for two-dimensional Dirac points in honeycomb photonic lattices in the paraxial approximation [2], in the context of so-called conical diffraction [2]. However, among the potential three-dimensional Weyl points, the unique spherical-shell expansion is most suitable to be observed in ultracold atomic gases. Depending on the initial excitation, the BEC shell could have some structure, which can be deduced by analogy with the fine structure of Poggendorff rings in optics [3].

III. SURFACE STATES AND FERMI ARCS

Weyl semimetals possess unusual topologically protected surface states in the form of 'Fermi arcs' in momentum space, as illustrated in Fig 3. Here we clarify in more detail calculations and interpretation around Fig 3. We consider a slab of our lattice cut orthogonally to the $\hat{x} - \hat{y}$ direction, and infinite along the $\hat{z}$ and $\hat{x} + \hat{y}$ directions. The slab has two surfaces (two planes), one is denoted as the left (L), and the other as the right (R) surface (see Fig. 3). The unit vectors of the Bravais lattice of the slab are $\mathbf{a}_1 = a(\hat{x} + \hat{y})$ and $\mathbf{a}_2 = a\hat{z}$. The Brillouin zone for the slab is two-dimensional, with reciprocal lattice unit vectors $\mathbf{b}_1 = \pi/a(\hat{x} + \hat{y})$ and $\mathbf{b}_2 = 2\pi/a\hat{z}$. There are N_p planes stacked along the finite direction of the slab ($\hat{x} - \hat{y}$). Thus, for every point in the Brillouin zone of the slab, $\mathbf{k} = k_{||}(\hat{x} + \hat{y})/\sqrt{2} + k_z\hat{z}$, there are N_p eigenstates. In Fig. 3(b) we plot the spectrum of these eigenstates, $E(\mathbf{k}) = E(k_{||}, k_z)$. The projections of the Weyl points of the 3D optical lattice on the $(k_{||}, k_z)$ plane are at $(k_{||}, k_z) = (\pm\pi/2\sqrt{2}a, \pm\pi/2a)$. For sufficiently large N_p, we clearly see [in Fig 3(b)] the spectrum corresponding to these four Weyl points. These energies at three-dimensional Weyl cones correspond to bulk states, not bound to the surface. In addition, there are two dispersion sheets in $E(\mathbf{k})$ corresponding to the surface states; one sheet corresponds to the left (L), and the other to the right (R) surface, as illustrated in

Fig. 3(b). These sheets intersect at 'Fermi arcs' [dashed lines in Fig. 3(b)], which connect the Weyl points of opposite chirality.

In the insets of Fig. 3 we plotted the profile of two eigenstates from the 'Fermi arcs' (we plot the absolute value squared of the wavefunction). When their momentum is distant from the momenta of the Weyl points, the state is completely bound on the surface. This can be seen in the right inset, corresponding to the state in the middle of the Fermi arc at ($k_{||} = 0$, $k_z = +0.99\pi/2a$). As the momentum of a 'Fermi arc' surface state approaches one of the Weyl points, the surface states join up with the bulk at positive and negative energies, and states strongly bound to the surface are lost (see Ref. [1] for detailed discussion on topological surface states). For example, the state at ($k_{||} = -0.95\pi/2\sqrt{2}a, k_z = +0.99\pi/2a$) plotted in the left inset extends far more into the bulk.

---

[1] A.M. Turner, A. Vishwanath, arXiv:1301.0330 (2013).

[2] O. Peleg, G. Bartal, B. Freedman, O. Manela, M. Segev, and D. N. Christodoulides, Phys. Rev. Lett **98**, 103901 (2007).

[3] M. V. Berry, J. Opt. A: Pure Appl. Opt. **6**, 289 (2004).